STUDIA UBB CHEMIA, LXV, 2, 2020 (p. 161-170)
(RECOMMENDED CITATION)
DOI:10.24193/subbchem.2020.2.13

THE INFLUENCE OF V_2O_5 ON SPECTROSCOPIC AND OPTICAL PROPERTIES OF MgO-KPO_3 GLASSES CO-DOPED WITH Ag_2O

CRISTINA SOMESAN[a], LIVIU CALIN BOLUNDUT[b*], LOREDANA OLAR[c*], VASILE POP[b], LEONTIN DAVID[a]

ABSTRACT. X-ray diffraction (XRD), Fourier transform infrared (FTIR), electron paramagnetic resonance (EPR), Ultraviolet-visible (UV-Vis) spectroscopies measurements have been employed to investigate the glasses from the $(V_2O_5)_x \cdot (KPO_3)_{80-x} \cdot (MgO)_{19} \cdot (Ag_2O)_1$ ($0 \le x \le 10$ mol%) system. The studied glasses had a fixed MgO and Ag_2O content of 19 mol% and 1 mol% respectively, and the V_2O_5:KPO_3 ratio was varied. XRD data confirms the vitreous nature of the studied samples. EPR, UV-Vis and IR data confirm the presence of vanadium in multiple valence states.

Keywords: *V_2O_5-MgO-KPO_3 glasses, X-ray diffraction, FT-IR, EPR, UV-vis analysis*

INTRODUCTION

During the last decades, glasses doped with transitional metal ions (TMI) have been the subject of many studies due to their interesting electrical, optical and magnetic properties which recommended them for potential application in many fields such as electrical memory switching, solid state lasers, phosphors, solar energy converters, catalysis and magnetic information storage, plasma display panels, electronic and optical devices [1-16]. Among different TMI, *vanadium ion* is considered extremely interesting due to the influences on some physical properties including electrical, optical, and

[a] *Babeş-Bolyai University, Faculty of Physics, Kogalniceanu str., Cluj-Napoca, Romania*
[b] *Technical University of Cluj-Napoca, Physics and Chemistry Depatment, 28 Memorandumului str., Cluj-Napoca, Romania*
[c] *University of Agiculture Sciences and Veterinary Medicine, 3-5 Calea Manastur, 400372 Cluj-Napoca, Romania*
** Corresponding authors: liviu.bolundut@chem.utcluj.ro, loredana.olar@usamvcluj.ro*

magnetic properties of the glasses [2, 7-10, 12-14]. In glasses and glass ceramics vanadium ions can exists in different oxidation states: +3 (trivalent), +4 (tetravalent) and +5 (pentavalent). In the glass network V^{3+} ions occupy octahedral symmetry, V^{4+} ions appear in both square pyramidal and octahedral position and V^{5+} ions can be found in tetrahedral, square pyramidal and octahedral configurations [13]. The 5+ (diamagnetic) and +4 (paramagnetic) are the most frequent valence states of vanadium ions in glasses [10]. The content of vanadium ions in different coordination and valence states in the glass depending upon the quantitative properties of modifiers and glass formers, size of the ions in the glass structure, their field strength, mobility of the modifier cation, etc. The simultaneous presence of vanadium ions in different valence states in glasses bring interesting changes in electrical characteristics. Thus, the semiconducting behaviour of glasses doped with vanadium ions is due by the hopping of unpaired $3d^1$ electron between V^{4+} and V^{5+} ions [2, 13, 14]. To be specific, it is quite possible for the intervalence transfer of electrons between these ions and contribute more to the electronic component of the electrical conductivity of the glasses. Also, the presence of vanadium ions in the studied glasses offers the possibility to investigate the local structure by electron paramagnetic resonance (EPR) spectroscopy [9, 10, 17, 18]. EPR spectroscopy is a very powerful tool in obtaining information regarding the local environment of TMI in the glass network and to identify the site symmetry around these ions [17-25].

On the other hand, in the last years exist a large degree of interest concerning glasses co-doped with silver oxide due to their high ionic conductivity and potential applications such as biomaterials with antibacterial and antimicrobial effects, laser optical data recording and photonics [5, 26-29].

The aim of this paper is to present our results obtained by means of XRD, FTIR, EPR and UV-Vis spectroscopies measurements performed on some potassium phosphate glasses gradually doped with vanadium ions and co-doped with a constant content of silver oxide. The research is part of a comparative analysis program focused on the behaviour of TMI in glasses, to obtain generally valuable rules, which allow imposing and controlling the properties of such materials.

RESULTS AND DISCUSSION

1. XRD and density data

XRD patterns of studied samples within Bragg angles from 10 to 70° at room temperature are presented in Figure 1. For all the investigated samples the XRD patterns exhibit few diffused scattering peaks at low angles instead of any

sharp peak indicating the amorphous nature of the studied samples. These amorphous nature features are characterized by three halos centred at 2θ ≈ 16°, 29° and 44°.

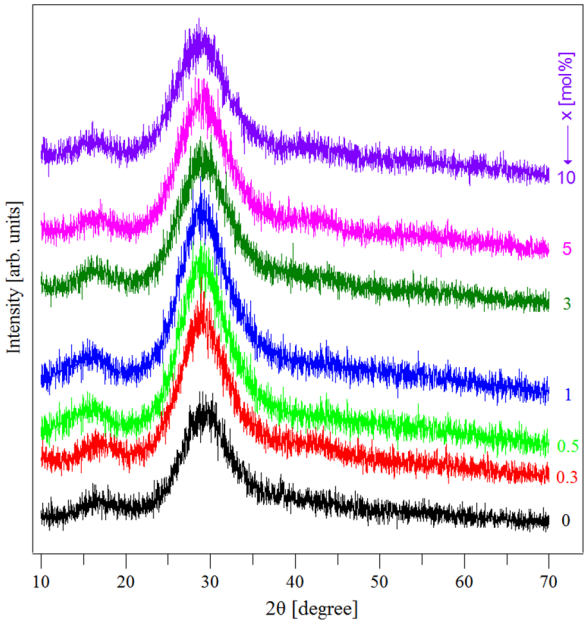

Figure 1. XRD patterns for the obtained samples

The compositional evolution of density for the studied glasses may provide important information concerning the possible structural changes that can occur in the host glass matrix by substitution of potassium metaphosphate by vanadium pentoxide. Figure 2 present the compositional dependence of the density for the studied glasses.

As can be seen from this figure the density increases with the increasing of V_2O_5 content in all the studies concentrations range. This evolution suggests that the increase of vanadium ions content in the studied glasses leads to a gradual inclusion of these ions in the host glass matrix. On the other hand, the non-linear compositional dependence of the density is due to the fact that the gradual addition of the vanadium ions leads not only to a simple incorporation of these ions in the host glass matrix but also generates structural changes in the glass network. Thus, the density data suggests that the vanadium ions play a network modifier role in the studied glasses.

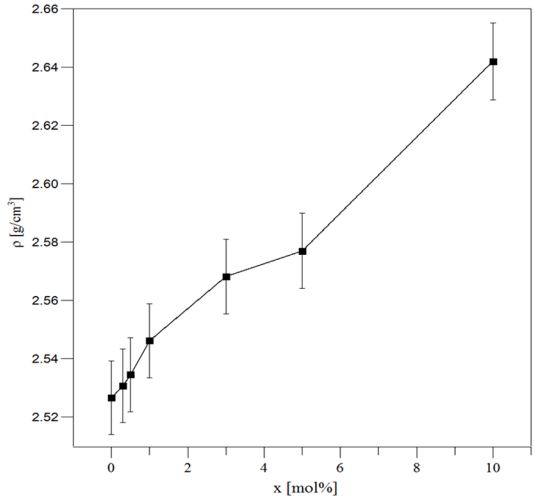

Figure 2. The density variation with the compositional evolution of the samples

2. FTIR data

Figure 3 present the FTIR spectra obtained for the studied glasses.

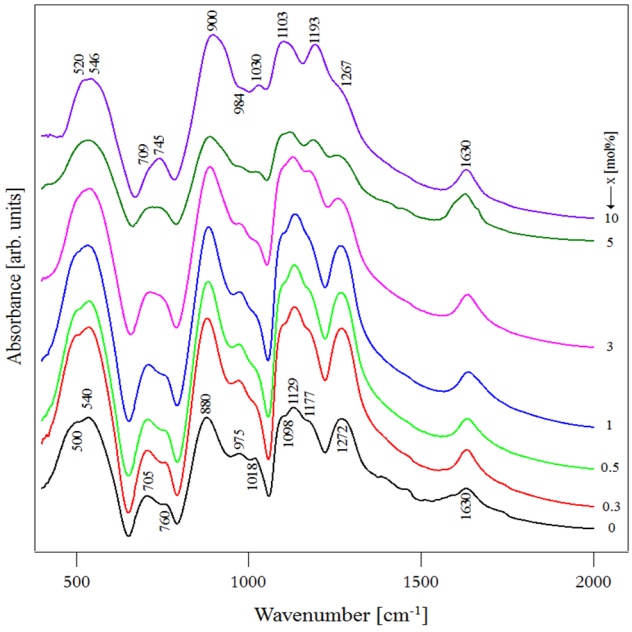

Figure 3. FTIR spectra for the studied samples

As can be observed the glass matrix and all the studied samples contain twelve absorption peaks in the range of 450-2000 cm^{-1} that can be assigned as follows, in accord with literature reports [19, 30-34]. Thus, the band from 500-520 cm^{-1} represent the bending vibration for P=O bonds in the case of matrix that is vanadium free, and bending modes for V-O-V bonds from the network that overlap with P=O vibration for the rest of the samples. The band from 540-546 cm^{-1} corresponding to the bending vibration in case of the O=P-O linkages. This band decrease when the concentration of the dopant (V_2O_5) increase. The behaviour is because the number of O=P-O bonds decrease (potassium monophosphate is replaced by vanadium pentoxide) and the number of V-O-V bonds increase. The first peak and the second form in the case of sample doped with 10 mol% of V_2O_5 an IR broad peak. The band from 705-709 cm^{-1} assigned to P-O-P symmetric stretching Q^2 type. 745-760 cm^{-1} represent the symmetric stretching vibration for P-O-P linkages. The band from 880-900 cm^{-1} assigned to asymmetric stretching vibration for P-O-P linkages from the glass network of matrix and for the rest of the samples is overlapped with symmetric vibrations of the V-O bonds from VO_4 tetrahedral that appear in the glass network when the dopant is added. The band from 975-984 cm^{-1} corresponds to the symmetric stretching vibration from $(PO_4)^{3-}$ group Q^0 type from the glass network. The band from 1018-1030 cm^{-1} for the matrix correspond to the asymmetric stretching vibration from $(PO_3)^{2-}$ groups, in the case of samples doped with vanadium can be assigned for the vibrations of V^{5+}=O double bond (in accord with UV-vis spectra that certifies the presence of pentavalent vanadium), also can correspond to the vibration of V-O bond from $[V_3O]$ groups or to the stretching of O-V-O bonds. The band from 1098-1103 cm^{-1} corresponds to the asymmetric stretching vibration from $(PO_4)^{3-}$ group Q^0 type. 1129 cm^{-1} assigned to the symmetric stretching vibration from $(PO_2)^-$ group Q^2 type from the glass network. The band from 1177-1193 cm^{-1} is due to the asymmetric stretching vibration from $(PO_2)^-$ group Q^2 type that built up the amorphous network. The band from 1267-1272 cm^{-1} can be assigned to the symmetric stretching vibration of P=O bonds from the glass network while the band of 1630 cm^{-1} correspond to water vibration.

3. UV-VIS data

UV-Vis data were obtained at room temperature being presented in Figure 4. The Figure 4 reveals the presence of four peaks for the sample doped with 10 mol% of V_2O_5 (two in the UV region and another two in visible region) and three for the rest of the studied samples.

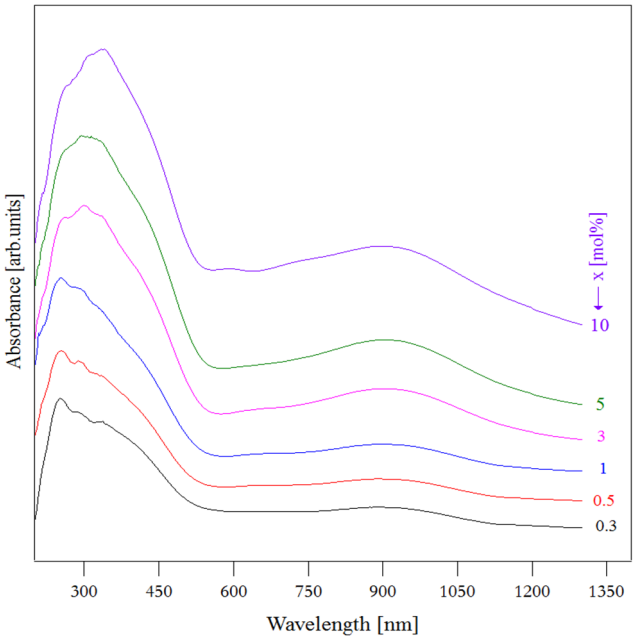

Figure 4. UV-vis spectra for samples from $(V_2O_5)_x \cdot (KPO_3)_{80-x} \cdot (MgO)_{19} \cdot (Ag_2O)_1$ ($0 \leq x \leq 10$ mol%) glass system

The samples were doped with V_2O_5 in this way the initial valence of vanadium is five. In glass according with the literature data [30], vanadium can exist in three different valence states V^{5+}, V^{4+}, V^{3+}. In the case of V^{5+} ion, the electronic structure is d^0 so the vanadium ion is incapable to give absorption peaks in the visible region of the optical spectrum because is not possible a d-d electronic transition (3d orbital being empty). But can be possible a charge transfer peaks that appear in UV region at about 290-340 nm according with the literature [31, 32] and confirmed by our results. It is interesting this behaviour, because phosphate glasses favour the presence of vanadium in low oxidation state (three and four) [31]. Our samples exhibit two charge transfer peaks in 285-340 nm region of the optical spectrum due to the presence of vanadium in highest oxidation state (V^{5+}).

In the visible region of the spectrum appears a very small peak at 597 nm. This peak it is observable only for the sample doped with 10 mol% of V_2O_5. According with other research data, this absorption can be attributed to the presence of vanadium in V^{3+} valence state [30], where vanadium is surrounded by six oxygen atoms in a distorted octahedral coordination. This absorption is due to $^3T_{1g}$ to $^3T_{2g}$ electronic transition.

Another peak in our case, for the studied samples appears at 930 nm. This absorption seems to be due to the presence of tetravalent vanadium as VO^{2+} in accord with other research data [30] and confirmed by our EPR data.

The intensity of absorption peaks increases when increase the concentration of the dopant (V_2O_5).

4. EPR data

To find more structural information related to the investigated system, EPR measurements were performed, at room temperature and the obtained spectra are illustrated in Figure 5.

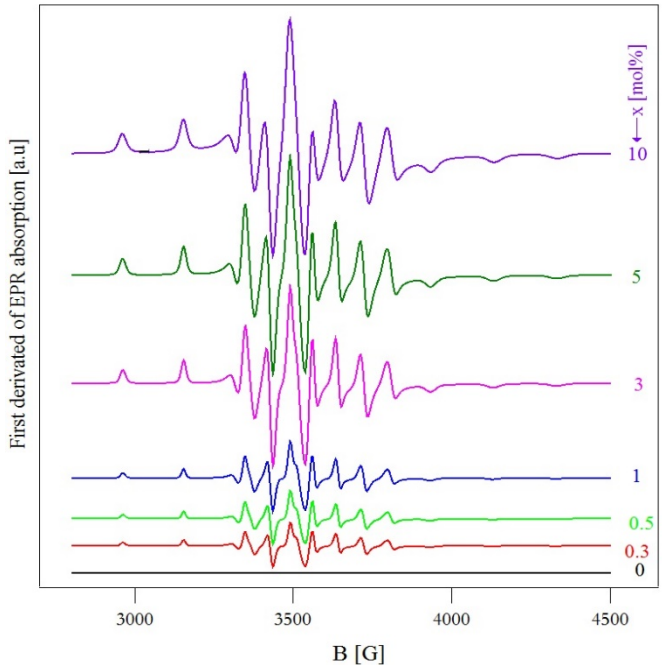

Figure 5. EPR data of the studied samples

The most significant finding in the EPR spectra, is the presence of the very well resolved hyperfine structure, with all features, for all prepared concentrations (up to x=10 %). These features are connected with very homogeneous distribution of the paramagnetic V^{4+} ions, which leads to very weak dipolar interactions or even to their absence.

Eight hyperfine lines (I=7/2) are expected for vanadyl (V^{4+}) ion in glasses, as a result of spin-orbit interaction in parallel band and same lines number in perpendicular one as the atom is aligned with field [35].

Other interesting result is the high ability of this system to incorporate V_2O_5 is the constant width of the hyperfine constant for all concentration ($A_{||}$ = 195 G)

The vanadium V^{4+} content increases constantly with V_2O_5 addition in the initial mixture, being illustrated by the increase in lines intensities, proving that during the melting process V^{5+} is reduced by the melting condition.

The V^{4+} ions built up vanadyl complexes with oxygen's from its neighbourhood and is located in octahedral field, with a tetragonal distortion, i.e. one V-O bond oriented axially, is shorter than the other [36]. Also, it was deduced from experimental data that, when the bond between the V^{4+} and on oxygen atom axially located is too long, caused by a lack in oxygen in the glass the complex can we considered as a pure tetrahedral one [37].

CONCLUSIONS

New samples from $(V_2O_5)_x \cdot (KPO_3)_{80-x} \cdot (MgO)_{19} \cdot (Ag_2O)_1$ ($0 \leq x \leq 10$ mol%) glass system were obtained.

XRD data confirm the amorphous state of the studied samples. The density measurement suggest that the vanadium ions play a network modifier role in our case.

IR and UV-vis data show the presence of vanadium in the glass network in multiple valence state.

EPR data also confirm the presence of V^{4+} ions in the glass network. So, all obtained data confirm the fact that at the working temperature a part of pentavalent vanadium is reduced to inferior oxidation states. Also, the vanadium ions seem to be octahedral surrounded by six oxygens fact confirmed by our obtained results.

EXPERIMENTAL SECTION

Glasses of the $(V_2O_5)_x \cdot (KPO_3)_{80-x} \cdot (MgO)_{19} \cdot (Ag_2O)_1$ ($0 \leq x \leq 10$ mol%) system were prepared by conventional melting and quenching method using V_2O_5, KH_2PO_4, MgO and Ag_2O of high purity (99.9%) in suitable proportion. The mechanically homogenized mixtures were melted in sintered corundum crucibles at 1100 °C for 10 minutes.

The X-Ray diffraction measurements of the samples were recorded with an XRD – 6000 Shimadzu diffractometer with a monochromator of graphite for Cu-Kα radiation (λ = 1.54060 Å) at room temperature.

The density of each sample was measured based on Archimedes principle at room temperature using toluene as immersing liquid. The samples were weighted on a KERN digital balance with an uncertainty of ± 0.00001 g.

The FTIR absorption spectra of the studied glasses and glass ceramics were obtained in the 360 - 1500 cm^{-1} spectral range with a resolution of 2 cm^{-1} using a JASCO FTIR 6200 spectrometer. The IR absorption measurements were done using the KBr pellet technique.

UV-VIS absorption spectra of the prepared samples were investigated with a JASCO V-550 spectrometer, in the wavelength range of 300-1380 nm having a resolution of 2 nm.

The EPR measurements of powder samples were carried out in the X-band (~ 9.79 GHz) at room temperature using a Bruker E-500 ELEXSYS spectrometer. The spectra processing was performed by Bruker Xepr software. To avoid the alteration of the glass structure due to the ambient conditions, especially humidity, samples were poured immediately after preparation and enclosed in tubular holders of the same calibre. The EPR spectra were recorded using equal quantities of samples.

REFERENCES

1. I. Ardelean; R. Ciceo-Lucacel; S. Filip; *J. Magn. Magn. Mater.*, **2004**, *272-276*, 337-338.
2. R. Balaji Rao; N.O. Gopal; N. Veeraiah; *J. Alloy Compd*., **2004**, *368*, 25-37.
3. I. Ardelean; S. Cora; R. Ciceo Lucacel; O. Hulpus; *J. Non-Cryst. Solids,* **2007**, *7*, 1438-1442.
4. Hirofumi Akamatsu; Katsuhisa Tanaka; Koji Fujita; Shunsuke Murai; *J. Magn. Magn. Mater.*, **2007**, *310*, 1506–1507.
5. R. Ciceo-Lucacel; I. Ardelean; *J. Non-Cryst. Solids*, **2007**, *53*, 2020–2024.
6. P. Bergo; W.M. Pontuschka; J.M. Prison; *Mater. Chem. Phys.*, **2008**, *108*, 142-146.
7. P. Pascuta; *J. Mater. Sci: Mater. Electron*., **2010**, *21*, 338-342.
8. H. Wen; P.A. Tanner; *J. Alloy Compd*., **2015**, *625*, 328-335.
9. G. Swapna; M. Upender; M. Prasad, *Optik,* **2016**, *127*, 10716-10726.
10. M. Montesso; D. Manzani; J. Donoso; C.J. Magon; I D.A. Silva; M. Chiesa; E. Morra; M. Nalin; *J. Non-Cryst. Solids*, **2018**, *500*, 133-140.

11. S. Kapoor; D. Brazete; I.C. Pereira; G. Bhatia; M. Kaur; L.F. Santos; D. Banerjee; A. Goel, J.M.F. Ferreira, *J. Non-Cryst. Solids*, **2019**, *506*, 98-108.
12. Sk. Jani Basha; M. Kostrzewa; A. Ingram; A. Siva Sesha Reddy; N. Purnachand; V. RaviKumar; M. Piasecki; N. Veeraiah; *J. Non-Cryst. Solids*, **2019**, *521*, 119529.
13. S. Das; A. Madheshiya; M. Ghosh; K. K. Dey; S. S. Gautam; J. Singh; R. Mishra; C. Gautam; *J. Phys. Chem. Solids*, **2019**, *126*, 17-26.
14. J. Fan; Y. Zhang; G. Li; Y. Yue; *J. Non-Cryst. Solids*, **2019**, *521*, 119491.
15. F.H. Margha; G.T. El-Bassyouni; G. M. Turky; *Ceram. Int.*, **2019**, *45*, 11838-11843.
16. L.C. Bolundut; V. Pop; *Studia UBB Chemia,* **2016**, *4*, 223-232.
17. J.L. Kumari; J.S. Kumar; S. Cole; *J. Non-Cryst. Solids*, **2011**, *357*, 3734-3739.
18. M. Rada; L. Rus; S. Rada; P. Pascuta; S. Stan; N. Dura; T. Rusu; E. Culea; *J. Non-Cryst. Solids*, **2015**, *414*, 59-65.
19. S. Bale; S.Rahman; *J. Non-Cryst. Solids*, **2009**, *355*, 2127-2133.
20. M. Subhadra; P. Kistaiah; *J. Non-Cryst. Solids*, **2011**, *357*, 3442-3446.
21. R. Stefan; P. Pascuta; A. Popa; O. Raita; E. Indrea; E. Culea; *J. Phys. Chem. Solids*, **2012**, *73*, 221-226.
22. T.D. AbdelAziz; N.A. Elalaily; F.M. Ezz-Eldin; J. Radiat; *Res. Appl. Sci.*, **2015**, *8*, 84-90.
23. V. Volpi; M. Montesso; S.J.L. Ribeiro; W.R. Viali; C.J. Magon; I.D.A. Silva; J.P. Donoso; M. Nalin; *J. Non-Cryst. Solids*, **2016**, *431*, 135-139.
24. R. Stefan; M. Karabulut; A. Popa; E. Culea; L. Bolundut; L. Olar; P. Pascuta; *J. Non-Cryst. Solids*, **2018**, *498*, 430-436.
25. C. Lin; J. Liu; L. Han; H. Gui; J. Song; C. Li; T.Liu; A. Lu; *J. Non-Cryst. Solids*, **2018**, *500*, 235-242.
26. J. Massera; Y. Shpotyuk; F. Sabatier; T. Jouan; C. Boussard-Plédel; C. Roiland; B. Bureau; L. Petit; N. G. Boetti; D. Milanese; L. Hupa; *J. Non-Cryst Solids*, **2015**, *425*, 52–60.
27. Y. Petit; K. Mishchik; N. Varkentina; N. Marquestaut; A. Royon; I. M. Honninger; T. Cardinal; L. Canioni; *Opt. Lett.*, **2015**, *40*, 4134-4137.
28. Y. Daiko; K. Segawa; S. Honda; Y. Iwamoto; *Solid State Ionics*, **2018**, *322*, 5-10.
29. A.A. Ahmed; A.A. Ali; A. El-Fiqi; *J. Mater. Res. Technol.*, **2019**, *8*, 1003-1013.
30. A.M. Abdelghany; A.H. Hammad; *Spectochim. Acta A*, **2015**, *137*, 39-44.
31. F.H. ElBatal; M.A. Marzouk; A.M. Abdelghany; *J. Non-Cryst. Solids*, **2011**, *357*, 1027-1036.
32. N. Laorodphan; P. Pooddee; P. Kidkhunthod; P. Kunthadee; W. Tapala; R. Puntharod; *J. Non-Cryst. Solids*, **2016**, *453*, 118-124.
33. P. Pascuta; G. Borodi; N. Jumate; I. Vida-Simiti; D. Viorel; E. Culea; *J. Alloy Compd.*, **2010**, *504*, 479-483.
34. D.A. Magdas; N.S. Vedeanu; D. Toloman; *J. Non-Cryst. Solids*, **2015**, *428*, 151-155.
35. D. Kivelson; S.K. Lee; *J. Chem. Phys.*, **1964**, *41*, 1896-1903.
36. D.L. Griscom; *J. Non-Cryst. Solids*, **1980**, *40*, 211-272.
37. N. Vedeanu; O. Cozar; I. Ardelean; B. Lendl; D. A. Magdas; *Vib. Spectrosc.*, **2008**, *48*, 259-262.